RESEARCH ARTICLE

3D Biosilica Scaffolds from *Melophlus sarasinorum* and *Xestospongia testudinaria* Indonesian Sponges are Biocompatible for Cell Growth and Differentiation of Human Wharton's Jelly Mesenchymal Stem Cell in Bone Tissue Engineering

Soraya Rahmanisa[1], Ekavianty Prajatelistia[2], Indra Wibowo[1], Anggraini Barlian[1,*]

[1]School of Life Sciences and Technology, Bandung Institute of Technology, Jl. Ganesha No.10, Bandung, 40132, Indonesia
[2]Faculty of Mechanical and Aerospace Engineering, Bandung Institute of Technology, Jl. Ganesha No.10, Bandung, 40132, Indonesia

*Corresponding author. E-mail: aang@sith.itb.ac.id

Received date: Apr 11, 2022; Revised date: Aug 15, 2022; Accepted date: Aug 16, 2022

Abstract

BACKGROUND: Biosilica derived from Indonesian marine sponge *Melophlus sarasinorum* and *Xestospongia testudinaria* is one of the biomaterials that can be developed together with synthetic polymer as a composite. Poly E-caprolactone (PCL) used as a composite role as an osteoconductive material together with biosilica and also tailored the slow rate of degradation in the body. This study aimed to create a biocompatible biosilica-based scaffold and supports osteogenic differentiation of human Wharton's Jelly mesenchymal stem cell (hWJ-MSCs).

METHODS: Biosilica was extracted from *M. sarasinorum* and *X. testudinaria* with the acid digestion method. Scaffold was prepared using the salt leaching method. The composite scaffolds were made from seven different biosilica extract and PCL. All of the scaffolds were tested for the cell morphology, Fourier-transform infrared spectroscopy (FTIR), immunocytochemistry, and cytotoxicity.

RESULTS: Composite scaffolds of 50% *M. sarasinorum* and *X. testudinaria* increased the cell viability and supported the cell growth within 14 days, whereas the osteogenic differentiation can be seen by the presence of collagen type 1 in day 12 based on immunocytochemistry result.

CONCLUSION: The biosilica scaffolds from PCL+50% *M. sarasinorum* and PCL+50% *X. testudinaria* were promising 3D scaffolds for potential application in bone tissue engineering. In conclusion, this study shows evidence for the osteogenic differentiation of hWJ-MSC, which might be developed for bone tissue engineering.

KEYWORDS: sponge, biosilica, scaffold, osteogenesis, stem cell

Indones Biomed J. 2022; 14(4): 382-92

Introduction

Bone damage is one of the leading causes of functional disorders caused by traumatic and pathological fractures, osteoporosis, joint and spinal fusion, revision arthroplasty, and plastic surgery that lead to repairing bone tissue structurally and physiologically. Some efforts are done to overcome this problem (1,2), including through tissue engineering. Bone tissue engineering is a technique that involves cells, biomaterials, and regulatory signals that play an essential role in the success of the technique.(3) Stem cells can be isolated from adipose tissue (4), bone marrow (5), skin (6), and umbilical cord (7). Stem cells isolated from the umbilical cord are so-called human Wharton's Jelly mesenchymal stem cells (hWJ-MSC). When compared to other stem cells, hWJ-MSC cells have several advantages, including easy to isolate, showing high proliferation rate, non-tumorigenic, and having allogenic properties.(8) MSCs are pluripotent stem cells that can be found in a variety of places throughout the body, including bone marrow, fat, vasculature, liver, and umbilical cord blood.(9-11) Three processes are involved in the formation of bone tissue: osteogenesis, modeling, and remodeling.

Osteogenesis is the transformation of undifferentiated cells or bone precursors into osteoblasts, which then differentiate into osteocytes. The osteoblast differentiation process is controlled by osteoblast-specific transcription factors, Runt-related transcription factor 2 (*runx2*) (12) and osterix (SP7) (13), in coordination with other transcription mediators, including collagen type 1 in the proliferation phase (day 0-7), *osteopontin* (*opn*) in maturation osteoblast (day 7-14), and *osteocalcin* (*ocn*), *sclerostin*, *dentin matrix acidic phosphoprotein* (DMP-1) in the osteocyte formation phase (day 14-21) of bone differentiation (14).

Biomaterial facilitate attachment, proliferation, differentiation of the cells, and the formation of specific organ tissues.(15) A scaffold is a three-dimensional structure that functions as a framework/template for cell growth and regulatory signals such as growth factors or biophysical stimuli for cell growth.(16) Many materials have been used to manufacture scaffolds, including metals,ceramics, polymers, and composites. However, there are some limitations to their use, especially the high manufacturing costs. To overcome these issues, natural materials have been shown to be a promising alternative for tissue engineering applications.(17) Natural materials can be derived from many sources, such as marine biomaterials and plant-based fibers (silk, collagen, hydroxyapatite) to fabricate this scaffold. Biosilica from marine sponges is being considered for biomedical approaches, bone replacement, and bone regeneration in tissue engineering, because silica ions are known as an important element to stimulate bone formation.

Biomaterials or scaffolds in tissue engineering are essential in providing structure and substrates for cells to attach, increase, and ultimately differentiate. Several literature studies have proven that silica plays a critical role in bone structure and function and is associated with bone calcium metabolism.(4-7) *In vitro*, *in vivo*, and clinical studies have demonstrated the ability of biosilica as a material for bone tissue engineerings, due to its high bioactivity, osteoconductivity, osteoinductivity, osteoconductivity, noncytotoxicity, nongenotoxicity, and antibacterial properties. Its outstanding biological and remarkable mechanical properties have made biosilica a promising bioceramic polymer for scaffold production. Biosilica scaffolds, which are made from Indonesian marine sponges whose bodies are porous and mostly made of calcium carbonate and silica, such as *Melopholus sarasinorum* and *Xestospongia testudinaria*, offer immense potential in supporting stem cell growth and facilitating cell differentiation.

Poly E-caprolactone (PCL), which has excellent biocompatibility, biodegradability, and mechanical strength, is a biodegradable polymer that can be used as an extracellular matrix (ECM) to help cells attachment.(8) Although PCL surface is hydrophobic, it can be modified by adding surface treatment to make it more hydrophilic for cell attachment and proliferation.(18) Another disadvantage of PCL is its lack of bone-forming properties, hence some studies tried to combined PCL with an osteogenic component, such as ceramics or bone morphogenetic proteins (BMPs), to promote osteogenesis.(19,20) PCL also does not promote the formation of blood vessels *in vivo*, which is essential for bone regeneration.(21) For a biomaterial to use in bone tissue engineering (BTE) applications, it must have high mechanical properties, slow degradation, osteoconductive and osteoinductive properties and should be capable of integrating with the surrounding bone tissue.(17) The high mechanical strength and slow degradation of PCL make it an ideal material for BTE.

The scaffold is the second component needed in tissue engineering technology. The scaffold acts as a synthetic matrix that imitates the natural matrix for the growth and development of cells. Biocompatible and biodegradable biomaterials are among the must-have scaffold criteria.(18,19) In tissue engineering, the scaffold is a three-dimensional structure that adapts to the body's *in vivo* environment. There haven't been many studies on the research of marine sponges, particularly the effect of biosilica in bone tissue engineering. Therefore, this study aimed to investigate the sponge's biosilica potential as a promising 3D scaffold for potential application in bone tissue engineering that can promote hWJ-MSC differentiation.

Methods

hWJ-MSCs Primary Cell Culture and Isolation

The stem cell that was used in this study was derived from the umbilical cord. Wharton's Jelly was obtained from Bandung Maternity Hospital, and the protocol of this study was approved by the same institution (No. KE-FK-0342-EC-2021). The sample was then cleaned in a 10% iodine solution. The primary culture of hWJ-MSCs was carried out by the enzymatic method. The umbilical cord sample was cut into pieces 3-5 cm in size, and veins and arteries were removed from the Wharton's Jelly. section. The Wharton's Jelly sections were cut to 1 cm x 1 cm, then placed in a 100 mm dish and incubated at room temperature to attach the tissue. The medium used in the primary culture consisted

of Dulbecco's medium, Low glucose Dulbecco's Modified Eagle's Medium (DMEM) (Thermo Fisher Scientific, Waltham, MA, USA), containing 10% Fetal Bovine Serum (FBS) (Thermo Fisher Scientific), and 1% antibiotic-antimitotic solution. The cell flask was incubated at 37°C of 5% CO_2, and the medium was changed every 2 days. When primary cells (P0) had reached 80% confluent, subcultures were carried out until they reached the end of passage 4 for further testing.(22)

Fabrication of Biosilica Scaffold from *M. sarasinorum* and *X. testudinaria*

The marine sponges used were *M. sarasinorum* and *X. testudinaria* that were extracted from the two species of Indonesian sponges that was used as the primary material for scaffold biomaterials for bone tissue engineering. The biosilica extract was carried out using the acid digestion method (23) as a mixture of the scaffold to be used. Sponges were extruded with HNO_3 and stirred for 1 hour; the residues were washed with equates until no color changed, and then repeated with the solution of H_2SO_4 and H_2O_2 ratio volume (1:1), the solution was stirred for 3 minutes and filtered the residues before the extract of biosilica could be used. (23) The scaffold was made using the salt leaching method, using a synthetic biomaterial composite (PCL), with various PCL concentrations.

There were seven composite scaffolds that were used in this experiment, as can be seen in Table 1. Scaffold fabrication using the salt leaching method (24,25) with a mixture of PCL as a non-organic polymer and commercial silica as a control scaffold. One gram of each biosilica and 1 gram of PCL were dissolved in 45 mL of chloroform, then stirred and heated until dissolved, added NaCl, and then poured into a round silicone mold with a diameter of 5 mm and 2 mm thickness, soaked in deionized water for 72 hours, 37°C, after that the scaffold washed and air-dried for 24 hours.

Scanning Electron Microscope (SEM) of hWJ-MSCs Grown on the Biosilica Scaffolds

SEM (SU3500, Hitachi, Tokyo, Japan) was used to observe the morphology and distribution of hWJ-MSC in the scaffold. The hWJ-MSC was grown on a biosilica scaffold for 24 hours at 37°C; of 5% CO_2. Cells were fixed by adding 100 µL 2.5 glutaraldehyde in 0.1 M cacodylate buffer, then incubated for 24 hours at 4ºC. The sample was further dehydrated with serial alcohol and then dried for 3 hours with a ratio of ethanol and HMDS (1:1). The sample was coated with gold (gold coating) and observed under SEM at 10 kV at 500 and 2000x magnification.

Fourier-transform Infrared Spectroscopy (FTIR) of the PCL and Biosilica Scaffold

FTIR analysis was performed on the PCL and biosilica scaffolds. FTIR spectrometer was used to detect chemical groups in the glass composition. Particle size distribution and morphology of the glass particles were also evaluated by a laser particle size analyzer (Fritsch Particle Size 'analysette 22, Fritsch International, Idar-Oberstein, Germany).(26)

Cytotoxicity Test of hWJ-MSC Grown on the Biosilica Scaffolds

Scaffold was cut into small pieces with 1 x 1 x 1 mm. Then the scaffold was sterilized with phosphate buffered saline (PBS) and UV before use and transferred to a 96 well plate, and the cells were planted for 24 hours. Cells were planted with a density of 5 x 10^3 cells for each scaffold. The medium was removed, added 10 µL of MTT solution in 90 µL of Low Glucose DMEM medium, cells were incubated at 37°C for 4 hours, dark room, for 4 hours, the MTT solution was discarded, and 100 µL of dimethyl sulfoxide (DMSO) was added. Cells were incubated for a maximum of 15 minutes in an incubator, room temperature or 37°C, and the absorbance was read with microplate reader at wavelength of 595 nm.(27)

Table 1. The ratio of composite scaffold for bone tissue engineering.

The Ratio of Composite Scaffold	Scaffold	Group Name of Composite Scaffolds
100% PCL	PCL	PCL
67% PCL : 33% pure silica	PCL ; silica 33%	PCL+Si33
50% PCL : 50% pure silica	PCL ; silica 50%	PCL+Si50
67% PCL : 33% biosilica *M. sarasinorum*	PCL ; MS 33%	PCL+MS33
50% PCL : 50% biosilica *M. sarasinorum*	PCL ; MS 50%	PCL+MS50
67% PCL : 33% biosilica *X. testudinaria*	PCL : XT 33%	PCL+XT33
50% PCL : 50% biosilica *X. testudinaria*	PCL ; XT 50%	PCL+XT50

Scaffold MTT Test

The MTT test observed the biocompatibility of the scaffold. As much as 5 x 10^3 hWJ-MSC cells were grown on each scaffold with dimensions of 5 x 5 x 2 mm, then Low Glucose DMEM growth medium was added, and incubated in a CO_2 incubator at temperature 37°C. Absorbance readings were carried out on days 1, 3, 5, 7, and 14. MTT readings were performed using a microplate reader (Bio-Rad, Hercules, CA, USA) with a wavelength of 570 nm.(28)

Collagen Type 1 Immunocytochemistry (ICC)

The attachment of hWJ-MSCs to the *M. sarasinorum* and *X. testudinaria* scaffolds was observed through the expression of collagen type. 1.5 x 10^3 cells grown on the scaffolds for 12 days. After 12 days, cell fixation was carried out with methanol, and then cells were rinsed with Tween-20 (0.05% in PBS). Blocking was done by adding BSA in PBST, then adding Anti-Collagen type 1 as primary antibody (Abcam, Cambridge, UK), secondary antibody in the form of goat anti-rabbit IgG HNL Alexa flour 488 (Cat No. ab150077, Abcam), and counterstaining with 4′,6-diamidino-2 -phenylindole (DAPI) (Thermo Fisher Scientific). The stained cells were then observed with an Olympus Fv 1200, confocal laser scanning microscope (Olympus, Tokyo, Japan).(29,30)

Statistical Analysis

Data obtained from all measurements (n=5) were analyzed by one-way ANOVA with statistical tools SPSS 22 (IBM Corporation, Armonk, NY, USA) and expressed as mean±standard deviation (SD). Statistical analysis results of the cytotoxicity study was carried out using ANOVA test followed by the Shapiro-Wilk test, with $p<0.05$ considered a significant result.

Results

Morphology of Scaffold

The morphological description of the scaffold used in this study was shown in Figure 1. The scaffold resulted in rounded pore shapes instead of squares, as seen in the standard NaCl crystal. This was due to the partial dissolution of NaCl surface in nitric acid. These phenomena were also found in the salt-leached scaffold prepared by the traditional dissolution. The color of the PCL scaffold was generally white, almost the same color as PCL+Si33 and PCL+Si50, whereas the biosilica scaffold from *M. sarasinorum* and *X. testudinaria* was generally seen as yellowish colored.

SEM Results of hWJ-MSC Grown on the *M. sarasinorum* Biosilica and *X. testudinaria* Biosilica Scaffold

Cell attachment on the surface of the scaffold was shown in Figure 2 after 24 hours of incubation. SEM in Figure 2 showed the surface morphology of the scaffolds and the cells. The presence of interconnected pores can be seen in the scaffold, which was essential for the passage of nutrition and dissolved oxygen for cell growth. Scaffolds that were overgrown with hWJ-MSC cells were shown by images of PCL+Si33, PCL+Si50, PCL+MS33, PCL+MS50, PCL+XT33, and PCL+XT50 on the right, while the PCL scaffolds was not ideal because it does not have a whole interconnected porous structure (Figure 2).

FTIR Results

Figure 3 showed the FTIR spectra of the PCL, and the composite of PCL and biosilica scaffolds that derived from *M. sarasinorum* and *X. testudinaria* sponges. The FTIR -ATR technique was performed to confirm the incorporation of the PCL matrix and its interaction with PCL matrix. Results shown in Figure 3 demonstrated that the FTIR adsorption spectrum of PCL showed the characteristic absorption peaks at 2817.23 cm^{-1} and 2943.17 cm^{-1}. The most intense peak at 1720 cm^{-1} was related to the carbonyl (C=O) stretching in the amorphous phase. The absorption peak at 1470 and 1365 cm^{-1} were due to the -CH bending of -CH_3 and OH in place bending vibrations respectively. According to Coleman and Zarian, the peak at 1292 cm^{-1} is assigned to the backbone C-C and C-O stretching in the crystalline phase of the PCL. Vibrations of the CH_2 group are found at 803.57 cm^{-1} and 500.76 cm^{-1} while peaks at 1728.91 cm^{-1} correspond to the

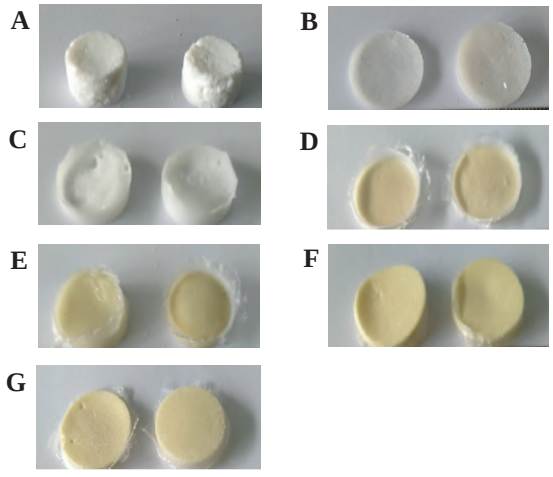

Figure 1. The morphology of various scaffolds created in this study. A: PCL; B: PCL+Si33; C: PCL+Si50l D: PCL+MS33; E: PCL+MS50, F: PCL+XT33, G: PCL+XT50. Size of scaffold (5 mm in diameter, 2 mm thickness) for all figures.

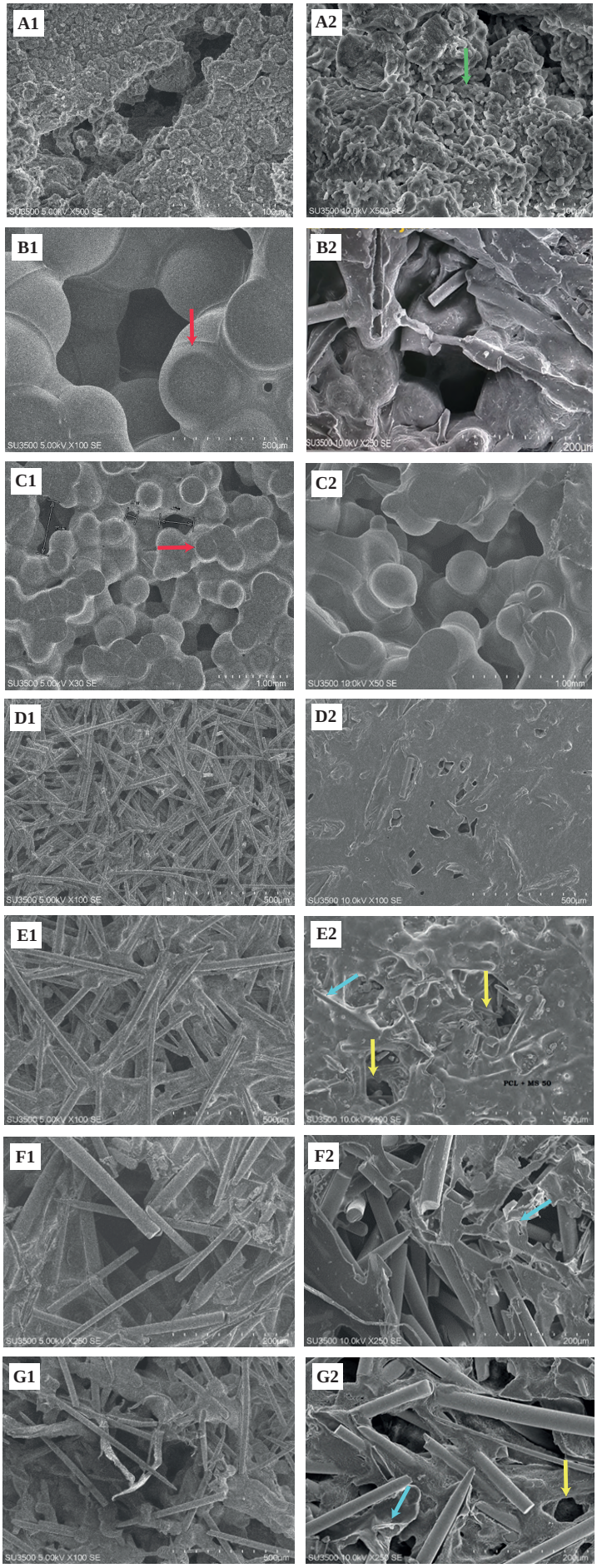

Figure 2. Attachment of hWJ-MSCs on fabricated scaffolds with various biosilica composition observed with SEM. A: PCL; B: PCL+Si33; C: PCL+Si50l D: PCL+MS33; E: PCL+MS50, F: PCL+XT33, G: PCL+XT50. Left (A1-G1): without cell; Right (A2-G2): seeded by cells after 24 h**.** Yellow arrow: interconnected pores); Green arrow: cell grown on the scaffold; Red arrow: pure silica; Blue arrow: filopodia.

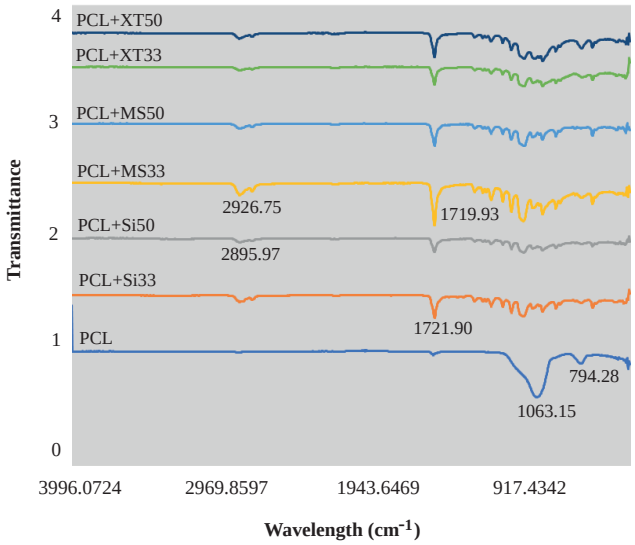

Figure 3. FTIR Spectra results of the PCL, composite of PCL+silica, and the composite of PCL+biosilica scaffolds that derived from *M. sarasinorum* and *X. testudinaria* sponges.

vibration of the C=O bond. Distinctive peaks at 1087.17 cm^{-1} are due to the stretching band of ester groups (C=H). The peak at 1728 cm^{-1} relates to C=O bonds and indicates the crystalline nature of synthesized PCL because, in the amorphous state, these bands appear at 1721.91 cm^{-1}.

FTIR adsorption spectrum of composite PCL+biosilica stretching mode of the carbonyl group (C=O) was observed at 1719.93 cm^{-1} and the peaks at 1163.72 cm^{-1} were respectively attributed to the symmetric stretching of C=H. Vibrations of the C-H group were found at 2895.97 cm^{-1}, which was showed the Si-O_2 bond, while peaks at 1721.98 cm^{-1} correspond to the vibration of the C=O bond. Distinctive peaks at 730.66 cm-1 were due to the stretching band of Si-O-Si groups. The peak at 1721.98 cm-1 was related to C=O bonds and indicating the crystalline nature of synthesized PCL, because in the amorphous state, these bands also appear at 1719.93 cm^{-1}.

Viability Test of hWJ-MSC Grown on Biosilica Scaffolds

Results showed that cells were viable on all scaffolds over the culture period. Most notably, cells were able to grow on the different scaffolds for the study duration. At early time points (24 hours), the metabolic activity for the PCL+XT33 composite was significantly difference compared to the PCL scaffold without biosilica, suggesting that combining the material of PCL and biosilica results in a composite scaffold with superior properties in terms of cell growth.

The viability study demonstrated that scaffolds with different concentrations of biosilica and PCL did not affect the cell viability of hWJ-MSCs after 72 hours (Figure 4). All groups of scaffolds did not affect the cell viability of hWJMSCs. Synthetic polymers, such as PCL, have biodegradable properties, support tissue regeneration and remodeling before being absorbed by the body, and are non-toxic. There were significant differences between the PCL+Si33 scaffold and the PCL+XT33 scaffold. The results of statistical analysis showed that cell viability was significantly different in the biosilica scaffold PCL+XT33 (p=0.045) and PCL+Si33 (p=0.027) when compared to PCL. The PCL+XT33 and PCL+XT50 scaffolds showed an increase in the viability of hWJ-MSC cells; this indicates that the biosilica contained in the scaffolds can support the viability and growth of hWJ-MSC cells and was not toxic to cells.

Scaffold Biocompatibility: Growth of hWJ-MSC

Figure 5 showed the graph of cell growth of hWJ-MSCs (OD=570 nm) on various scaffolds for 14 days of treatment, PCL+MS33 and PCL+XT50 had the highest OD values. Statistical results showed a significant difference between the PCL+XT50 compared to PCL+Si50, PCL+MS33 was significantly different from PCL+Si33, and PCL+XT50 was significantly different when compared to PCL, PCL+Si50, PCL+MS50, and PCL+XT33 (p<0.05). Also in the group of PCL+MS33, the statistical result showed a significant difference to PCL, PCL+Si50, PCL+MS50, and PCL+XT33 (p<0.05) Scaffold PCL+MS50 had significant mean difference compare to scaffold group PCL, PCL+Si33, PCL+Si50, and PCL+XT50 (p<0.05). PCL+XT33 was also showed a significant difference compared to PCL, PCL+Si33, PCL+MS33, and PCL+XT50.

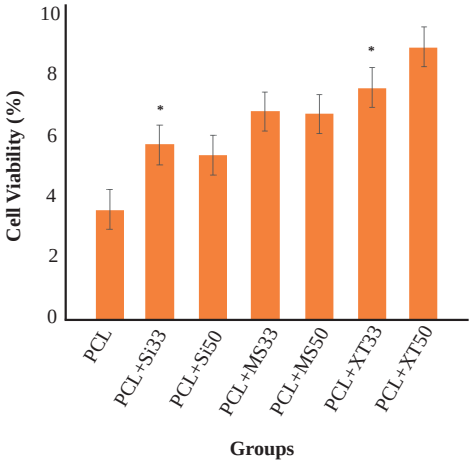

Figure 4. Cell viability of the scaffolds. Each column represents the mean±SE between the samples. Each group showed an increase in cell viability and nontoxicity to the cell. *p<0.05 was considered significant when being compared to PCL group.

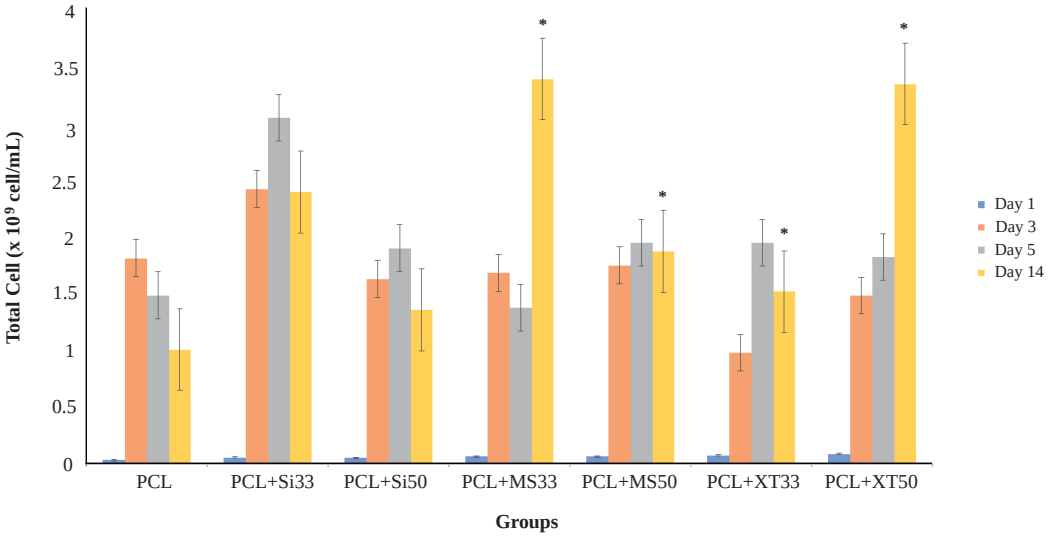

Figure 5. Graph of cell growth of hWJ-MSCs (OD=570 nm, 1 OD is equal to 1 x 10^9 cells/mL) on various scaffolds for 14 days of treatment. PCL+XT50 group was significantly different from PCL+Si50, PCL+MS33 group was significantly different from PCL+Si33 group, and PCL+XT50 group was significantly different when compared to PCL, PCL+Si50, PCL+MS50, and PCL+XT33 groups. *p<0.05 was considered statistically significant.

Biosilica from *X. testudinaria* (PCL+XT50) and from *M. sarasinorum* (PCL+MS33) scaffolds showed the best cell proliferation activity among observed scaffolds on day 14. We assumed that most of the hWJ-MSCs attached, proliferated, and differentiated within the scaffold. The MTT activity results demonstrated an increase in the cell's metabolic activity after 3 and 5 days of culture. A scaffold was considered toxic if it inhibits more than 50% of cell proliferation. The least inhibitory value means the scaffold was not toxic. This indicated that the materials tested (PCL and biosilica composites) were non-cytotoxic and able to support the attachment, proliferation, and viability of hWJ-MSCs.

Collagen Type 1 Expression

Type 1 collagen expression of hWJ-MSC cells was observed by ICC staining. For 12 days, 5 x 10^3 cells were grown on the scaffold. After 12 days of treatment, cells were fixed with methanol and washed with Tween-20 (0.05% in PBS). The expression of type 1 collagen (green fluorescence staining) was indicated by red arrows (Figure 6). Type 1 collagen was expressed most clearly from the confocal microscope image on the combination of scaffolds PCL+MS33 (Figure 6C), PCL+MS50 (Figure 6D), PCL+XT33 (Figure 6E), PCL+XT50 (Figure 6F), and when compared to scaffolds PCL+Si33 (Figure 6A) and PCL+Si50 (Figure 6B), and the PCL scaffold (Figure 6G). To confirm that the cell penetrates into the scaffold, the 3D pictures were captured (Figure 6H, Figure 6I).

Discussion

A scaffold should possess interconnected porous architecture, porosity, controlled degradation, and enough mechanical strength to withstand the pressure exerted by the proliferating and differentiating cells both *in vitro* and *in vivo*.(31) Furthermore, biocompatibility is a crucial property that should be provided by the scaffold. Topical advances in tissue engineering have led to the development of a scaffold with ideal properties by using composites or blends. Slow degradation and less biocompatibility will restrict the usage of these synthetic polymers in tissue engineering so as PCL.(32) PCL as a composite with biosilica was used to increase the osteoconductivity of bone scaffold and mimic the condition of the cell proliferation and adhesion.(32)

The attachment of cells inside the scaffold surface is shown in Figure 2 after 24 hours of incubation. At 100X magnification, hWJ-MSCs are spread evenly over the scaffold surface and pore as seen in Figure 2A(PCL), Figure 2B (PCL+Si33), Figure 2C (PCL+Si50), Figure 2D, (PCL+MS33), Figure 2E (PCL+MS50), Figure 2F (PCL+XT33), and Figure 2G (PCL+XT50). Cells that were seeded into scaffolds cover the more surface area in PCL+MS33, PCL+MS50, and PCL+XT33 than in the PCL, PCL+Si33, & PCL+Si50 scaffolds. The cells in the PCL scaffold appear spherical, whereas the cells in the biosilica scaffold show a more elongated morphology with filopodia. SEM results suggest that cells grown on scaffolds with

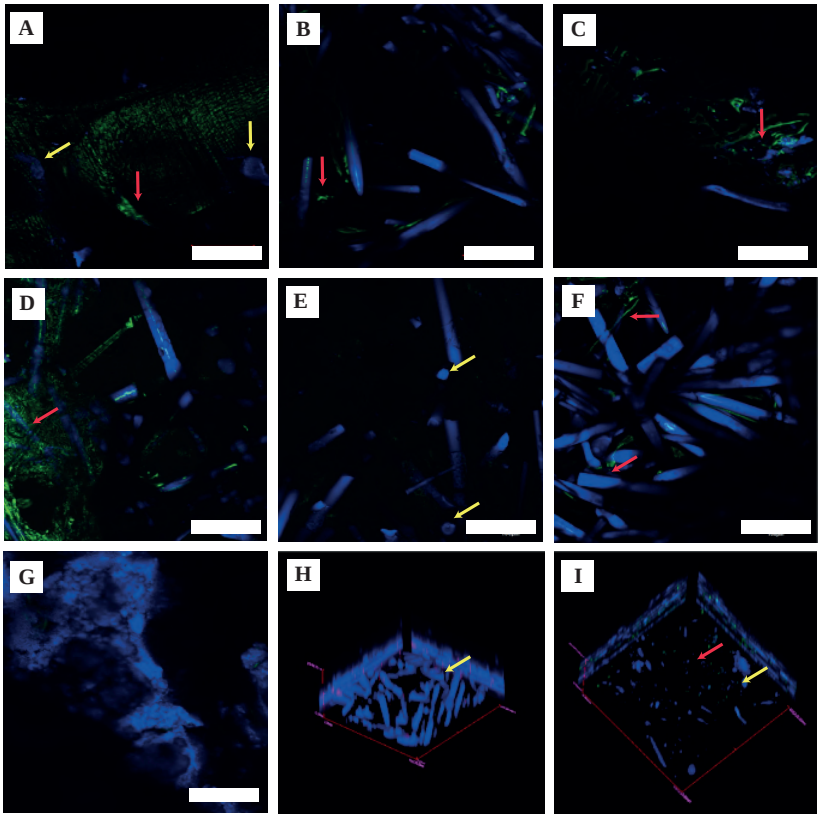

Figure 6. ICC staining for type I collagen (green) within the scaffold over 12days of culture (n=3). A: PCL+Si33; B: PCL+Si50; C: PCL+MS33; D: PCL+MS50; E: PCL+XT33; F: PCL+XT50; G: PCL; H: PCL+XT50 (in 3D), I: PCL+MS50 (in 3D). Yellow arrow: cell nuclei stained with DAPI; Red arrow: collagen type 1. White bar: 100 µm.

biosilica from *X. testudinaria* and *M. sarasinorum* were able to enhance the cell spreading stage. This stage plays an critical role in supporting cell proliferation as well as cell differentiation. Scaffolds with biosilica from sponges with hWJ-MSCs can accelerate the cell's growth due to the medium's diffusion in the interconnected pore gaps that allow cells to migrate. For bone scaffold, the criteria should preferably be osteo-inductive, osteo-conductive, and osteo-integration. Biosilica scaffold has shown massive potential for bone tissue engineering application because one of the criteria which is biocompatible; hence, the scaffold should have similar mechanical properties to the bone tissues. The scaffold is not only able to act as a media or matrix for cellular adhesion but is also able to support and promote new tissue formation.(32) The role of biosilica in this study suggested that biosilica had promoted the proliferation of hWJ-MSCs in the scaffold. Biosilica from species *X. testudinaria* has a role as an osteoconductor for the initiation of bone proliferation.(33)

The overall growth of hWJ-MSC (Figure 5) on PCL+MS33 and PCL+XT50 scaffolds continued to increase for 14 days compared to PCL and pure silica scaffolds. These results indicate that all scaffolds were biocompatible for hWJ-MSCs. The main advantage of this PCL polymer lies in the ability to adjust the mechanical strength. It is possible to control the rate of degradation in the fabrication of the scaffold from this synthetic polymer, which has good biocompatibility but poor mechanical properties, accelerated material degradation in samples with higher biosilica percentages, which can affect the release of ions from biosilica, which is a stimulus for cell differentiation. This result is consistent with the higher bioactivity of biosilica scaffolds compared to PCL and commercial silica. The scaffold observed by SEM supported the attachment and proliferation of the hWJ-MSCs to the surface of the biosilica scaffold. The formation of the multilayer structure starts with this extracellular matrix sheet. Because of the short incubation time (24 hours), hWJMSC cells have a strong affinity for the biosilica scaffold surface.(7)

The spectrum of PCL showed the characteristic bands at 1087.17 and 803.57 cm^{-1}, due to the asymmetric and symmetric C-H and CH2 stretching vibration. The characteristic bands of PCL which were described in Figure 3 are also found in their pastes in addition to the stretching vibration of COC- groups of the biosilica ingredient which is presented at 1180 cm^{-1}. Compared to the PCL, which have the spectrum around 1500-2000 cm^{-1} revealed the characteristic of C=C, C=O, and C=N stretching bands (34), the spectrum of biosilica revealed the characteristic Si-O-C stretching bands at 1200 cm^{-1} (symmetric) and 1100 cm^{-1}

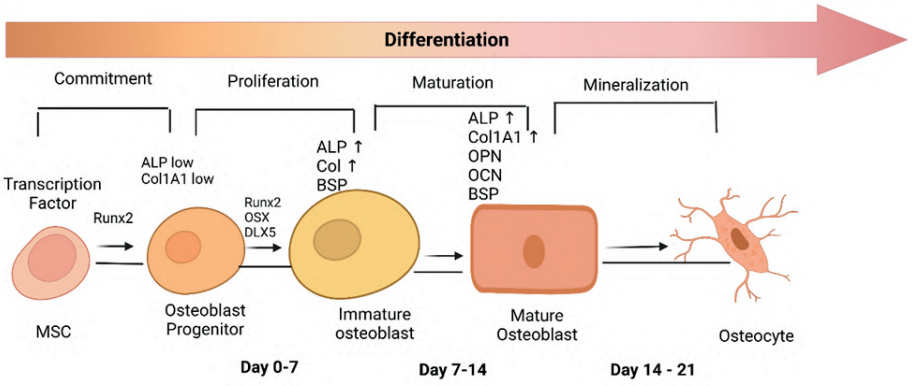

Figure 7. Expression of osteogenic markers during osteogenesis differentiation. The runx2 is highly expressed in immature osteoblast and down-regulated in mature osteoblast. *Runx2* initiated the expression of *opn*, *ocn*, *sclerostin*, and DMP-1 in the day 14 (mineralization stage) (Created with BioRender.com).

(asymmetric). Furthermore, there were hydroxyl groups in the spectrum from PCL+XT50, Amide A (N-H) stretching bands presented in 2000-2500 cm^{-1}.(35-37)

Cell penetration and proliferation to the scaffold qualitatively visualized by Confocal Laser Scanning Microscope had started on day 12 of culture (Figure 6). To confirm the cell penetration into the biosilica scaffold, the image was taken by Z stacking image (Figure 6H, Figure 6I). The expression of collagen type 1 (red arrow) based on the confocal image in the PCL scaffold after 12 days was fewer cells than cells grown on scaffold mixed with biosilica (*M. sarasinorum* and *X. testudinariain* the PCL+MS50, PCL+XT30, and PCL+XT50 scaffold. The expression of collagen type 1 ended in day 14. The cells were able to penetrate from the upper surface of the scaffold to the lower surface of the scaffold. Based on these results (qualitatively), a scaffold with biosilica especially from marine sponges specific could support the attachment of cells to the surface of the scaffold. In this *in vitro* study there was no addition of growth factor in the medium for cell differentiation, this study suggests that the combination of PCL and biosilica scaffold, can be appropriate for bone tissue engineering, however, further experiments need to be conducted to confirm the stability of the bone using those combinations in the *in vivo* study.

An increased of mRNA level of these genes (*runx2*, *opn*, and collagen type 1) were seen between days 7-14 of differentiation (Figure 7). *Runx2* is a transcriptional factor in osteogenic differentiation and essential for chondrocyte maturation. During osteoblast differentiation, *runx2* is weakly expressed in immature osteoblast, and reaches the maximum level in the late phase of immature osteoblasts, and is down-regulated in mature osteoblasts.(17) *Runx2* target genes include *opn*, collagen type 1, *ocn*, *sclerostin*, and DMP-1.(38)

The result of this study showed that the composite scaffold PCL+MS50 and PCL+XT50 support the osteogenic differentiation of hWJ-MSC, it can be proved from the result of expression of collagen type 1 from ICC on the stage of mature osteoblast (day 12) which is in line with the level at stage mature osteoblast (day 7-14). *Runx2* as a master of regulator gene and control the expression of collagen type 1 in osteoblast differentiation.(38)

Conclusion

The study results demonstrated that the biosilica scaffold is biocompatible and supports the growth of hWJ-MSCs cells on the scaffold. Among seven composite scaffolds, PCL+MS50 and PCL+XT50 support the growth of hWJ-MSC cells on the scaffold. The biosilica scaffolds PCL+MS50 and PCL+XT50 that fabricated from the two species of Indonesian sponges, *M. sarasinorum* and *X. testudinaria* was a promising 3D scaffold for potential application in bone tissue engineering.

Acknowledgements

The authors thank the Prodia Education and Research Institute (PERI) Grant for supporting this research, and Hutomo Tanoto and Safira Medina, who have carefully prepared the sponge extraction.

Authors Contribution

AB, EP, and IW were involved in planning and supervised the work. SR processed the experimental data, performed

the analysis, drafted the manuscript and designed the figures. AB aided in the interpretation of the results and worked on the manuscript. All authors discussed the results and commented on the manuscript.

References

1. Meiliana A, Dewi NM, Wijaya A. In search for anti-aging strategy: can we rejuvenate our aging stem cells? Indones Biomed J. 2015; 7(2): 57-72.
2. Ikawati M, Ertanto Y, Endah ES, Pudjiraharti S, Meiyanto E, Jenie RI. Anti-osteoporosis potencies of Zingiber officinale Rosc. rhizome water extract and DFA III produced from Dahlia spp. L.: in vivo and in vitro studies. Indones Biomed J. 2022; 14(1): 104-15.
3. Judawisastra H, Nugraha FR, Wibowo UA. Porous architecture evaluation of silk fibroin scaffold from direct dissolution salt leaching method. Macromol Symp. 2020; 391(1): 1900187. doi: 10.1002/masy.201900187.
4. Gao C, Peng S, Feng P, Shuai C. Bone biomaterials and interactions with stem cells. Bone Res. 2017 Dec 21; 5: 17059. doi: 10.1038/boneres.2017.59.
5. Müller WEG, Schröder HC, Feng Q, Schlossmacher U, Link T, Wang X. Development of a morphogenetically active scaffold for three-dimensional growth of bone cells: Biosilica-alginate hydrogel for SaOS-2 cell cultivation. J Tissue Eng Regen Med, 9: E39– E50. doi: 10.1002/term.1745.
6. Fernandes KR, Magri AMP, Kido HW, Ueno F, Assis L, Fernandes KPS, et al. Characterization and biological evaluation of the introduction of PLGA into biosilicate. J Biomed Mater Res Part B 2017: 105B: 1063-74.
7. Fernandes KR, Parisi JR, Magri AMP, Kido HW, Gabbai-Armelin PR, Fortulan CA, *et al.* Influence of the incorporation of marine spongin into a Biosilicate®: an in vitro study. J Mater Sci Mater Med. 2019; 30: 64. doi: 10.1007/s10856-019-6266-2.
8. Jeon HJ, Lee MJ, Yun SH, Kang DG, Park KH, Choi SJ, *et al.* Fabrication and characterization of 3D-printed biocomposite scaffolds based on PCL and silanated silica particles for bone tissue regeneration. Chem Eng Sci. 2019; 360: 519-30.
9. Marlina M, Rahmadian R, Armenia A, Widowati W, Rizal R, Kusuma HSW, *et al*. Isolation, characterization, proliferation and differentiation of synovial membrane-derived mesenchymal stem cells (SM-MSCs) from osteoarthritis patients. Mol Cell Biomed Sci. 2020; 4(2): 76-82.
10. Meiliana A, Dewi NM, Wijaya A. Mesenchymal stem cells manage endogenous tissue regeneration. Indones Biomed J. 2016; 8(2): 61-70.
11. Darmayanti S, Triana R, Chouw A, Dewi NM. Is stem cell a curer or an obstruction? Mol Cell Biomed Sci. 2017; 1(1): 17-27.
12. Kaur K, Das S, Ghosh S. Regulation of human osteoblast-to-osteocyte differentiation by direct-write 3D microperiodic hydroxyapatite scaffolds. ACS Omega. 2019; 4(1): 1504-15.
13. Amable PR, Teixeira MVT, Carias RBV, Granjeiro JM, Borojevic R. Identification of appropriate reference genes for human mesenchymal cells during expansion and differentiation. PLoS One. 2013; 8(9): 0073792. doi: 10.1371/journal.pone.0073792.
14. Rutkovskiy A, Stensløkken KO, Vaage IJ. Osteoblast differentiation at a glance. Med Sci Monit Basic Res. 2016; 22: 95-106.
15. Yin S, Zhang W, Zhang Z, Jiang X. Recent advances in scaffold design and material for vascularized tissue-engineered bone regeneration.Adv Healthc Mater. 2019; 8(10): 201801433. doi: 10.1002/adhm.201801433.
16. Bassi G, Panseri S, Dozio SM, Sandri M, Campodoni E, Dapporto M, *et al.* Scaffold-based 3D cellular models mimicking the heterogeneity of osteosarcoma stem cell niche. Sci Rep. 2020; 10: 22294. doi: 10.1038/s41598-020-79448-y.
17. Park BW, Kang EJ, Byun JH, Son MG, Kim HJ, Hah YS, *et al.* In vitro and in vivo osteogenesis of human mesenchymal stem cells derived from skin, bone marrow and dental follicle tissues. Differentiation. 2012; 83(5): 249-59.
18. Granito RN, Custódio MR, Rennó ACM. Natural marine sponges for bone tissue engineering: The state of art and future perspectives. J Biomed Mater Res B Appl Biomater. 2017; 105(6): 1717-27.
19. Palamà IE, Arcadio V, D'Amone S, Biasiucci M, Gigli G, Cortese B. Therapeutic PCL scaffold for reparation of resected osteosarcoma defect. Sci Rep. 2017; 7: 12672. doi: 10.1038/s41598-017-12824-3.
20. Eltom A, Zhong G, Muhammad A. Scaffold techniques and designs in tissue engineering functions and purposes: A review. Adv Mater Sci. Eng. 2019; 2019: 3429527. doi: 10.1155/2019/3429527.
21. Sadiasa A, Nguyen TH, Lee BT. In vitro and in vivo evaluation of porous PCL-PLLA 3D polymer scaffolds fabricated via salt leaching method for bone tissue engineering applications. J Biomater Sci Polym Ed. 2014; 25(2): 150-67.
22. Amsar RM, Barlian A, Judawisastra H, Wibowo UA, Karina K. Cell penetration and chondrogenic differentiation of human adipose derived stem cells on 3D scaffold. Future Sci OA. 2021; 7(8): FSO734. doi: 10.2144/fsoa-2021-0040.
23. de Barros IB, Volkmer-Ribeiro C, da Veiga Junior VF, Silva CC. Extraction of high purity silica from Amazonian sponges. J Bioprocess Biotech. 2016; 6: 4. doi: 10.4172/2155-9821.1000276.
24. Cannillo V, Chiellini F, Fabbri P, Sola A. Production of Bioglass® 45S5 - Polycaprolactone composite scaffolds via salt-leaching. Compos Struct. 2010; 92(8): 1823-3.
25. Pezeshki Modaress M, Mirzadeh H, Zandi M. Fabrication of a porous wall and higher interconnectivity scaffold comprising gelatin/chitosan via combination of salt-leaching and lyophilization methods. Iran Polym J. 2012; 21: 191-200.
26. Ghassemi T, Shahroodi A, Ebrahimzadeh MH, Mousavian A, Movaffagh J, Moradi A. Current concepts in scaffolding for bone tissue engineering. Arch Bone Jt Surg. 2018; 6(2): 90-99.
27. Gabbai-Armelin PR, Kido HW, Cruz MA, Prado JPS, Avanzi IR, Custódio MR, *et al.* Characterization and cytotoxicity evaluation of a marine sponge biosilica. Mar Biotechnol. 2019; 21(1): 65-75.
28. Dwivedi R, Kumar S, Pandey R, Mahajan A, Nandana D, Katti DS, *et al.* Polycaprolactone as biomaterial for bone scaffolds: Review of literature. J Oral Biol Craniofac Res. 2020; 10(1): 381-8.
29. Zaitseva OV, Shandrenko SG, Veliky MM. Biochemical markers of bone collagen type I metabolism. Ukr Biochem J. 2015; 87(1): 21-32.
30. Akhir HM, Teoh PL. Collagen type I promotes osteogenic differentiation of amniotic membrane-derived mesenchymal stromal cells in basal and induction media. Biosci Rep. 2020; 40(12): BSR20201325. doi: 10.1042/BSR20201325.
31. O'brien FJ. Biomaterials and scaffolds for tissue engineering. Mater Today. 2011; 14(3): 88-95.
32. Sultana N, Khan TH. Polycaprolactone scaffolds and hydroxyapatite/polycaprolactone composite scaffolds for bone tissue engineering," J Bionanosci. 2013; 7 (2): 169-73.

33. Wang X, Schröder HC, Wiens M, Schloßmacher U, Müller WE. Biosilica: Molecular biology, biochemistry and function in demosponges as well as its applied aspects for tissue engineering. Adv Mar Biol. 2012; 62: 231-71.
34. Wiens M, Niem T, Elkhooly TA, Steffen R, Neumann S, Schloßmacher U, *et al.* Osteogenic potential of a biosilica-coated P(UDMA-co-MPS) copolymer. J Mater Chem B. 2013; 1(27): 3339-43.
35. Borhan S, Hesaraki S, Behnamghader AA, Ghasemi E. Rheological evaluations and in vitro studies of injectable bioactive glass-polycaprolactone-sodium alginate composites. J Mater Sci Mater Med. 2016; 27(9): 137. doi: 10.1007/s10856-016-5745-y.
36. Gentile P, McColgan-Bannon K, Gianone NC, Sefat F, Dalgarno K, Ferreira AM. Biosynthetic PCL-graft-collagen bulk material for tissue engineering applications. Materials (Basel). 2017; 10(7): 693. doi: 10.3390/ma10070693.
37. Nandiyanto ABD, Oktiani R, Ragadhita R. How to read and interpret ftir spectroscope of organic material. Indones J Sci Technol. 2019; 4(1): 97-118.
38. Rutkovskiy A, Stensløkken KO, Vaage IJ. Osteoblast differentiation at a glance. Med Sci Monit Basic Res. 2016; 22: 95-106.